Electrical and microstructural characterization of molybdenum tungsten electrodes using a combinatorial thin film sputtering technique

Seung-Ik Jun[a] and Philip D. Rack
Department of Materials Science and Engineering, The University of Tennessee, Knoxville, Tennessee 37996-2200

Timothy E. McKnight, Anatoli V. Melechko, and Michael L. Simpson
Molecular Scale Engineering and Nanoscale Technologies Research Group, Oak Ridge National Laboratory, Oak Ridge, Tennessee 37831

(Received 8 October 2004; accepted 13 December 2004; published online 15 February 2005)

A combinatorial rf magnetron sputter deposition technique was employed to investigate the electrical characteristics and microstructural properties of molybdenum tungsten (MoW) high temperature electrodes as a function of the binary composition. In addition to the composition, the effect of substrate bias and temperature was investigated. The electrical resistivity of MoW samples deposited at room temperature with zero bias followed the typical Nordheim's rule as a function of composition. The resistivity increases with tungsten fraction and is a maximum around 0.5 atomic fraction of tungsten. A metastable β-W phase was identified and the relative amount of the β-W phase scales with the resistivity. Samples deposited at higher temperature (250 °C) also followed Nordheim's rule as a function of composition, however, it did not contain the metastable β-W phase and consequently had a lower resistivity. The resistivity of samples deposited with substrate bias is uniformly lower and obeyed the rule of mixtures as a function of composition. The molybdenum-rich compositions had a lower resistivity, contrary to expectations based on bulk resistivity values, and is attributed to high electron-dislocation scattering cross sections in tungsten versus molybdenum. The metastable β-W phase was not observed in the biased films even when deposited at room temperature. High resolution scanning electron microscopy revealed a more dense structure for the biased films, which is correlated to the significantly lower film resistivity. © *2005 American Institute of Physics*. [DOI: 10.1063/1.1855395]

I. INTRODUCTION

Thin film transistors (TFTs) have been widely studied because of their electronic switching capability and have applications for electronic display devices, MEMS (Micro Electro Mechanical Systems), optoelectronic (image) sensors, and chemical/biological sensors.[1] For TFTs to achieve high-speed, high-density, and low-power consumption, a low-resistivity gate and/or source-drain metal electrode is essential. As shown in Table I, molybdenum (Mo) (and Mo alloys), aluminum (Al) (and Al alloys), and copper (Cu) are generally used as gate electrodes in manufacturing electronic displays and semiconductor devices. In choosing a metal material for the gate electrodes, there is a trade-off between resistivity and thermal/chemical stability. Al and Cu, for example, have very low electrical resistivity and therefore have a significant advantage and attraction to applications in high-speed and large-scaled thin film devices. However, their thermal stability is very poor, especially for processing temperatures in excess of 500 °C. One of the main problems occurs during heat treatment of the Al (Cu)–Si contact because Al (or Cu)–Si interdiffusion is significant above 500 °C. This interdiffusion can, for example, create silicon precipitates in Al which reduces the overall conductivity of the lines. In addition, Al can suffer from electromigration which is a metal mass transport due to an electric current. Al atoms move in the direction of electron flow, toward the anode, and vacancies remain in the Al thin film. Consequently, Al whisker growth can be observed between Al and Si films. If the whiskers contact other layers, for example dielectric layers, they can cause additional device failures. When Al is passivated by a dielectric, hillock formation can cause cracking of such films. To prevent hillock formation, in the case of using Al as a gate electrode, a Mo layer can be added to form a Mo/Al bilayer.[2] The bilayer deposition and dry etch processes, however, are more complicated. The dry etch process is particularly difficult because the Mo and Al etch chemistries are different.

When fabricating TFT devices, the etching profile of the gate electrode is also very important. This is especially true for an invert-staggered TFT structure where the gate electrode is the bottom layer (typically used in TFT-liquid crystal displays). These structures require a tapered etch profile for several reasons. First, it provides better step coverage in subsequent deposition patterning processes. Second, the sharp edged (undercut) gate is a main source of dielectric breakdown due to the concentration of electric field at this sharp-edged point. Third, the tapered gate electrodes influence the electrical properties of TFT and can lower threshold voltages and facilitate steep swing characteristics.

For the past several years, the molybdenum tungsten (MoW) alloy has been studied and used as gate electrodes for

[a]Electronic mail: sjun3@utk.edu

TABLE I. Representative gate electrode materials for fabrication of thin film transistors.

Material	Resistivity ($\mu\Omega$ cm)	Stress resistance	Taper angle in dry etching
MoTa	40–45	Excellent	Good
MoW	15–20 (Conventional)	Excellent	Excellent
	7–10 (Our work)		
Al alloy (AlNd)	5–7 (post-annealed)	Fair	Good (AlNd)
Al–Cu	4–5	Fair	Fair
Al	4–5	Poor	Fair
Cu	3–4	Good	Fair

thin film transistor–liquid crystal displays (TFT-LCD) manufacturing companies because of its excellent thermal and chemical stability, reasonably low resistivity, and easily controllable etch taper angle.[3,4] In spite of its excellent properties, problems with larger substrate size and higher device driving speed have been encountered. Some of the problems include flicker, cross talking, and line delay due to relatively high resistivity of MoW (15–20 $\mu\Omega$ cm). To compensate the high resistance, MoW thin films require wider and thicker patterns. The wider and thicker MoW causes some fabrication problems in large-scaled integration and planarization of the device which can also lead to device failure. Therefore a thorough investigation of the process-property relationships of the MoW alloy is necessary to extend the utility of this alloy to advanced semiconductor applications. Although MoW has many advantages in microelectronics, especially high temperature applications, there is not much published work on this thin film alloy. In this work, we present electrical and microstructural properties as a function of the MoW composition for films sputtered under various conditions (temperature and bias).

II. EXPERIMENTAL DETAILS

The details of the sputtering conditions used to deposit the MoW specimens are shown in Table II. An AJA ATC2000 rf magnetron sputtering system equipped with heated and dc biased substrate holder was utilized for the deposition of Mo, W, and MoW thin films (Fig. 1). The films were deposited on thermally oxidized $SiO_2(1\ \mu m)/Si(100)$ substrates. The substrate holder can be rotated if uniform thickness and composition are desired and produces a $Mo_{1-x}W_x(0.1<x<0.9)$ gradient when the sample is not rotated (combinatorial mode). As shown in Fig. 1, the system has three targets each equipped with rf matching network and supply. The sources can be tilted and the *z* position of the substrate holder can be varied *in situ* to change the deposition profile. The sputtering targets have a 50 mm diameter and a 6 mm thickness. The base pressure prior to the sputtering deposition was below 5.0×10^{-6} Pa and the total flow rate of argon used in the sputtering was fixed at 25 SCCM (SCCM—cubic centimeter per minute at STP) for all conditions. The substrate is heated by quartz lamps and the temperature is controlled within ±1 °C temperature range. The resistance was analyzed via four point probes (Veeco FPP-5000) at a fixed film thickness (~300 nm) and the reported value is an average of at least three measurements over the sample. The film thickness was evaluated by using Surface Profiler (KLA Tencor Alpha-Step 500). The crystal structure characteristics of the films were analyzed with a Phillips X-pert Pro x-ray diffraction (XRD) system, and the microstructure was analyzed by using a Hitachi S-4700 scanning electron microscope (SEM). The first series was designed to analyze electrical properties and microstructures as a function of Mo–W composition, applied bias, and substrate temperature. The second series was designed to explore the effects of the applied bias on the electrical and microstructural properties of MoW.

TABLE II. Experimental description of this work. Fixed parameters: 25 sccm Ar gas, 70 mm gap between substrate and target.

		rf power (W)				
Run no.	ID	Mo	W	dc bias (W/V)	Pressure (Pa)	Temperature (°C)
1st series	(a)	200	160	0/0	0.66	RT
	(b)	200	160	0/0	0.66	250
	(c)	200	160	30/165	0.66	RT
	(d)	200	160	30/165	0.66	250
2nd series	(a)	200	0	0/0	1.06	RT
	(b)	200	0	15/140	1.06	RT
	(c)	200	0	30/165	1.06	RT
	(d)	200	0	45/190	1.06	RT
	(e)	0	200	0/0	1.06	RT
	(e)	0	200	15/140	1.06	RT
	(f)	0	200	30/165	1.06	RT
	(g)	0	200	45/190	1.06	RT
	(h)	200	200	0/0	1.06	RT
	(i)	200	200	15/140	1.06	RT
	(j)	200	200	30/165	1.06	RT
	(k)	200	200	45/190	1.06	RT

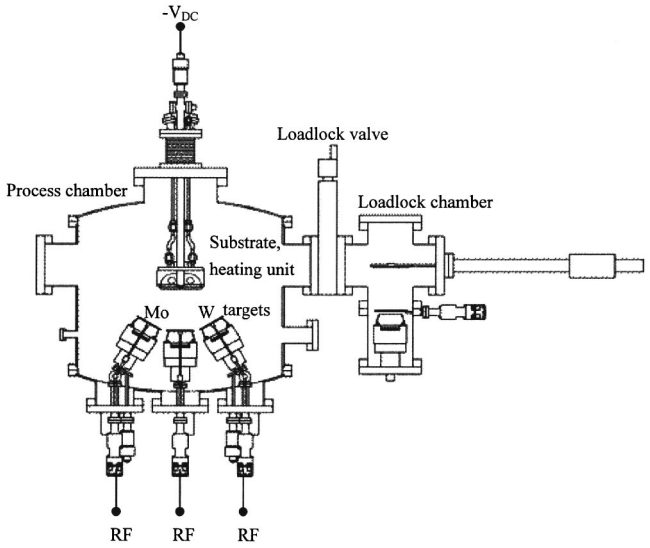

FIG. 1. Schematic diagram of an AJA ATC2000 rf magnetron sputtering system equipped with dc bias supply.

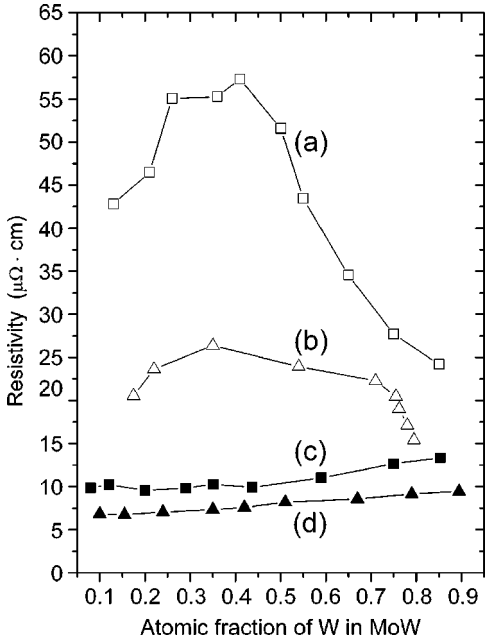

FIG. 2. Electrical resistivity of MoW as a function of composition, temperature, applied bias, and process pressure: (a) no bias, RT; (b) no bias, 250 °C; (c) 30 W (165 V) bias, RT; and (d) 30 W (165 V) bias, 250 °C; from the 1st series.

III. RESULTS AND DISCUSSION

A. Films deposited without negative bias at room temperature and 250 °C

The electrical resistivity of the MoW alloy as a function of atomic fraction of W is shown in Fig. 2. Figures 2(a) and 2(c) are processed under room temperature and Figs. 2(b) and 2(d) are under 250 °C. And Figs. 2(a) and 2(b) are processed without bias and Figs. 2(c) and 2(d) are under a 30 W (165 V) dc bias. The resistivity results as a function of W fraction for (a) and (b) samples that are processed without bias follow typical Nordheim's relationship. In a metallic material, the electron scattering due to the perturbations such as solute atoms, second phases, impurities, dislocations, vacancies, and grain boundaries increase electrical resistivity. As demonstrated in Fig. 2, the electrical resistivity of the MoW binary system increases with increasing solute concentration, and it has the maximum at ~0.5 atomic fraction of solute atoms because of high electron scattering due to defects from mixing of the solid solution. The resistivity of binary alloys can be expressed by the well-known Nordheim's equation

$$\rho_I = Cx(1-x), \tag{1}$$

where x is the fraction of solute atoms and C is Nordheim coefficient. This expression is valid for binary systems having the same valency. Therefore, the total resistivity of the metal alloy can be described with Matthiessen's rule

$$\rho = \rho_T + \rho_R + \rho_I. \tag{2}$$

Combining Eqs. (1) and (2) yields

$$\rho = \rho_T + \rho_R + Cx(1-x), \tag{3}$$

where ρ_T is the resistivity due to scattering from thermally activated vibration; ρ_R is the residual resistivity due to the scattering from crystal defects, dislocations, vacancies, and impurities, etc.; and ρ_I is the resistivity arising from solute atoms.

The Nordheim coefficients of (a) and (b) in Fig. 2 are 118 and 70 $\mu\Omega$ cm, respectively. The sputtering temperature provides energy to the arriving species which enhances their surface mobility and allows the species to occupy a lower energy state. This leads to a more ordered structure which reduces the electron scattering and lowers the electrical resistivity.

Figure 3 shows XRD results of MoW as a function of W fraction at several sputtering conditions; (a) room temperature with no bias, (b) room temperature with 30 W (165 V) bias, 250 °C with no bias, and 250 °C with 30 W (165 V) bias. The XRD result of Fig. 3(b) is identically shown in RT/30 W bias, 250 °C/no bias, and 250 °C/30 W bias sputtering conditions. In the XRD spectra, the strong peak around $2\theta=40°$ is a confluence of several peaks from α-W (40.26°, 110 plane), β-W (39.89°, 210 plane), and Mo (40.51°, 110 plane). The weak peak around $2\theta=38°$ is a noise signal from the aluminum sample holder. As shown in Fig. 3(a), at room temperature and without bias, a second metastable phase (β-W) is observed which correlates well with the resistivity, i.e., higher β-W content correlates with higher resistivity. The intensity of β-W (200) changes significantly with the atomic fraction of W in MoW alloy and has a maximum at ~0.5 W. We opine that the β-W fraction in MoW is highest at the ~0.5 W composition because the strain induced by the lattice mismatch between Mo and W is highest at ~0.5 W which helps nucleate the metastable β-W. The β-W has a 5.05 Å lattice constant and its lattice mismatch with α-W is about 37.3% in transforming from β-W to stable α-W phase. It has an A15 crystal structure and W atoms are positioned at (0, 0, 0), $(\frac{1}{2},\frac{1}{2},\frac{1}{2})$, $(\frac{1}{4},\frac{1}{2},0)$, $(\frac{3}{4},\frac{1}{2},0)$, $(0,\frac{1}{4},\frac{1}{2})$, $(0,\frac{3}{4},\frac{1}{2})$, $(\frac{1}{2},0,\frac{1}{4})$, and $(\frac{1}{2},0,\frac{3}{4})$ sites.[5] It appears that the presence of metastable β-W causes electron scattering which increases the electrical resistivity of the

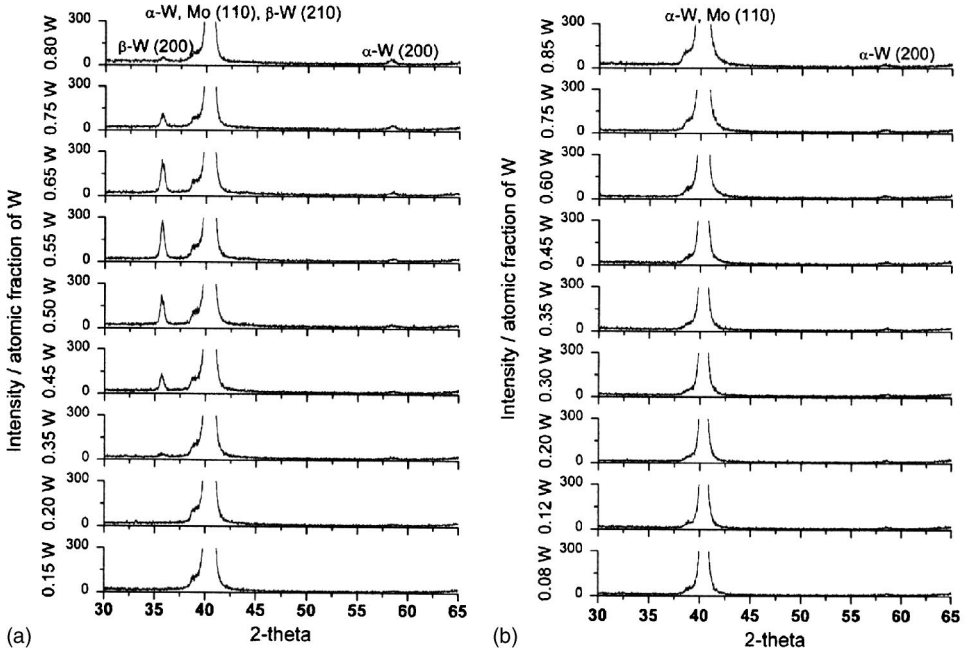

FIG. 3. XRD spectra results of MoW as a function of W atomic fraction at the condition of (a) RT/no bias, (b) RT/30 W bias, 250 °C/no bias, and 250 °C/30 W bias.

MoW thin film. The relationship between the amount of β-W from the XRD results and electrical resistivity of the MoW is shown in Fig. 4. The relative amount of β-W to α-W is calculated from the intensities of the (200) planes located at 58.27° (α-W) and 35.52° (β-W), respectively, and compared to the intensities expected from the standard diffraction patterns of each phase. This iteration was used because the (200) planes were the only peaks that did not have significant overlap with any other peaks.

For the room temperature and unbiased sputter deposited sample, Fig. 4 shows that the presence of the second phase β-W significantly affects the resistivity. As the XRD peak intensity of β-W increases, the electrical resistivity also increases and has a maximum value at the point of ~0.5 atomic fraction W.

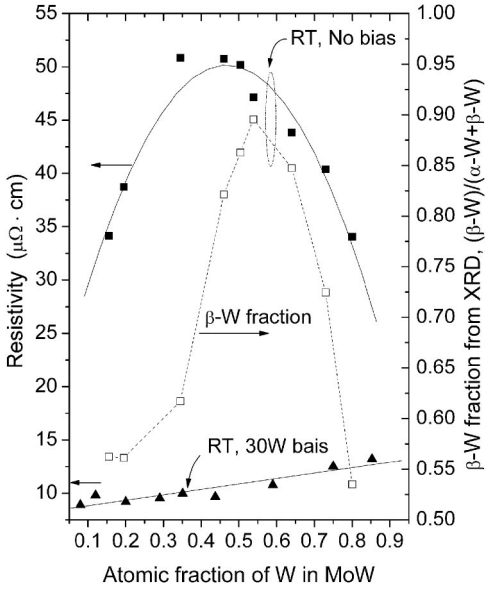

FIG. 4. The relationship between β-W fraction and electrical properties of MoW as a function of composition (The β-W fraction at room temperature/30 W bias is zero because β-W phase is not present under all biased sputtering conditions even at room temperature sputtering).

The sample deposited at 250 °C and unbiased does not contain the β-W phase over the entire composition range as illustrated in Fig. 3(b). This correlates to Fig. 2(c) which shows that resistivity of the 250 °C sample decreases relative to the room temperature deposited sample. This decrease is well correlated to the elimination of the second phase β-W. The higher temperature deposition could also induce a slightly more ordered lattice with fewer lattice defects which could also contribute to the lower resistivity. This contribution is not expected to be significant, however, due to the refractory properties of this alloy system. Therefore, the major factor that the 250 °C *in situ* heating has on the MoW film is to slightly order the material and inhibit the metastable β-W phase from forming.

B. Films deposited with negative bias (30 W, −165 V) at room temperature and 250 °C

Comparing Figs. 2(a) and 2(b) to Figs. 2(c) and 2(d), respectively, illustrates the effect that substrate bias has on the MoW alloy resistivity. A significant reduction in the film resistivity over the entire composition range is realized for each condition. Unlike the unbiased samples, however, the resistivity of the biased samples do not follow Nordheim's rule. Rather, these samples obey a rule of mixtures relationship $\rho_{\mathrm{MoW}}=x_{\mathrm{Mo}}\rho_{\mathrm{Mo}}+x_{\mathrm{W}}\rho_{\mathrm{W}}$ as a function of W fraction in MoW as shown in Fig. 2(c) and 2(d). In this case the following relationship applies:

$$\rho = \rho_T + \rho_R + (x_{\mathrm{Mo}}\rho_{\mathrm{Mo}} + x_{\mathrm{W}}\rho_{\mathrm{W}}), \tag{4}$$

where x_{Mo} and x_{W} are atomic fraction of Mo and W, respectively, and ρ_{Mo} and ρ_{W} are the resistivity of Mo and W, respectively.

With bias sputtering of ~30 W (−165 V), the metastable β-W is not present, even at room temperature as shown in Fig. 3(b). Figure 5 shows a series of SEM images as a function of the tungsten fraction for samples deposited at room temperature with and without substrate bias. From the figure,

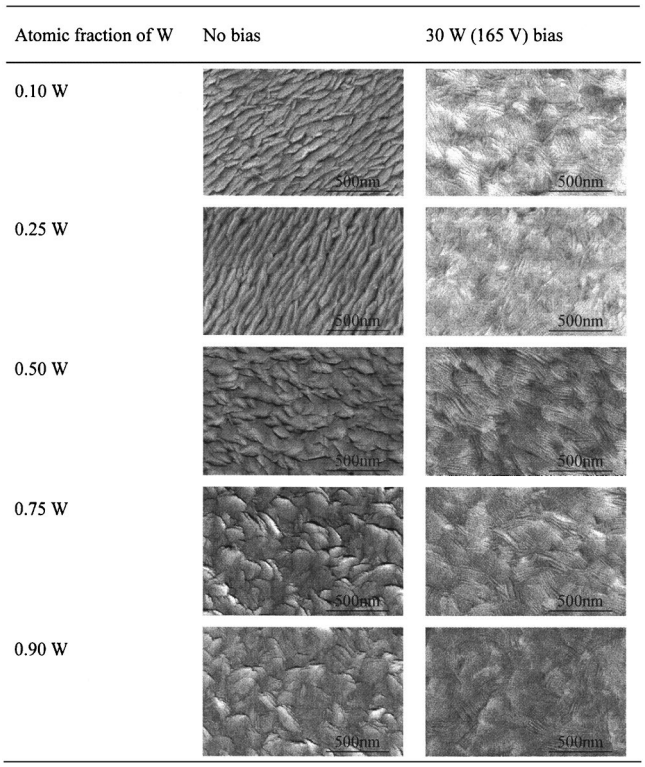

FIG. 5. SEM images of MoW surface morphology as a function of the W atomic fraction in MoW thin films for samples deposited at room temperature with and without substrate bias.

it can be seen that the biased microstructure is denser and has less void space between grains. Table III illustrates the effect that substrate bias has on the lattice constant measured normal to the substrate. The substrate bias increases the lattice parameter of the MoW alloy and qualitatively it is shown that the induced strain in the *z* direction is a result in a change in the biaxial stress in the plane of the substrate which is tensile without substrate bias and compressive with substrate bias. While the magnitude of the stress was not specifically determined, thicker (1 μm) thick MoW films deposited with substrate bias peeled off subsequent to deposition, whereas unbiased 1 μm thick films did not.

Another interesting observation from Figs. 2 and 4 is that the biased tungsten-rich alloy has a higher resistivity than biased molybdenum-rich alloy, (c) and (d). It is well known that the resistivity of bulk tungsten (α-W, 5.49 $\mu\Omega$ cm) is slightly lower than that of molybdenum (Mo, 5.78 $\mu\Omega$ cm) at room temperature. The reason for the higher resistivity for the tungsten-rich end of the biased samples can be explained by the dislocation density of tungsten relative to molybdenum. Shukovsky and co-workers showed that the dislocation resistivity of tungsten is higher than that of molybdenum. Specifically, the dislocation resistivity of tungsten and molybdenum are reported to be 6.7×10^{-11} and 5.8×10^{-13} $\mu\Omega\,\mathrm{cm}^3$, respectively.[6–8] During sputtering deposition on a biased substrate, the deposited MoW film is subjected to ion bombardment by highly energized ions and these ions can produce ion-radiated defects such as dislocation loops and point defects.[5] The electron scattering from dislocations in tungsten is nearly two orders of magnitude higher than molybdenum; therefore the tungsten-rich MoW alloy has a higher resistivity than the molybdenum-rich alloy. While the dislocation density in the films increases the resistivity of the tungsten-rich end, the overall effect of substrate bias improves the resistivity of the entire alloy. The substrate bias inhibits the β-W alloy from forming and produces a much denser film structure. While dislocations are likely generated by the impinging energetic species, the lattice structure has fewer vacancies and a more ordered overall structure.

In order to survey thermal stability of MoW (0.35 atomic fraction W), we investigated the current density and breakdown voltage of SiO_2 thin film with MoW electrodes after annealing up to 700 °C by using current-voltage measurement. The structure of these samples is MoW/PECVD SiO_2/Si (100) and it was vacuum annealed at 100 °C to 700 °C (the upper limit of system) in 100 °C increments for 1 h. There were no changes in the current den-

TABLE III. Result summary of the 2nd series. (Fixed parameters: 0.66 Pa, room temperature, 25 sccm Ar gas, 70 mm electrodes-gap.)

	Applied bias [W (V)]	Resistivity $\mu\Omega$ cm	Deposition rate (nm/min)	XRD (110) 2θ	Lattice[a] constant (nm)
Mo	0	42.9	5.16	40.59	0.3141
	15 (140 V)	13.0	3.36	40.33	0.3161
	30 (165 V)	11.9	3.97	40.33	0.3162
	45 (190 V)	12.6	3.61	40.33	0.3161
W	0	18.7	5.50	40.37	0.3157
	15	13.1	4.43	40.17	0.3172
	30	13.1	4.16	40.15	0.3173
	45	14.8	3.64	40.15	0.3173
MoW[b]	0	55.5	11.59	40.46	0.3150
	15	11.6	7.32	40.29	0.3163
	30	12.7	7.57	40.29	0.3163
	45	12.9	7.13	40.28	0.3164

[a]Lattice constant of α phase.
[b]0.5 atomic fraction of W.

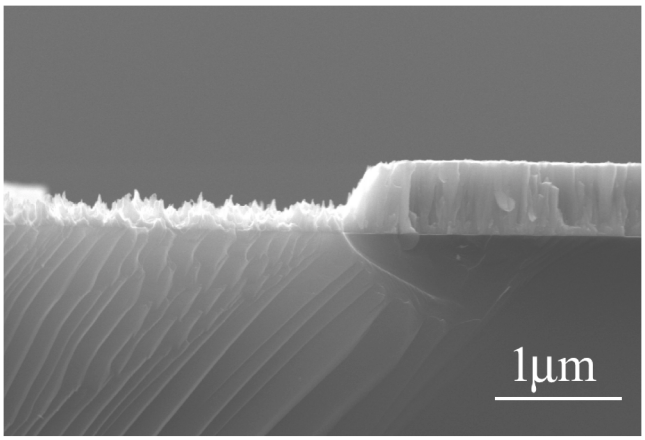

FIG. 6. Dry etching profile of MoW (0.35 atomic fraction of W) just before end point etching (reactive ion etching, 120 W rf power, 16 Pa pressure, $SF_6/O_2=25/35$ sccm).

sity and breakdown voltage between the as-deposited and annealed samples up to 700 °C which confirms the excellent high-temperature stability of MoW electrodes.

Figure 6 shows dry etching profile of MoW (0.35 atomic fraction of W). An Trion Technologies Oracle reactive ion etching (RIE) system was used and the sample was etched under the process conditions of 120 W rf power, 16 Pa pressure, SF_6/O_2 (25/35 sccm) gas flow rate. The etch profile is shown just before end point etching. This profile shows a slight tapered angle ($\sim 80°$) which can be significantly reduced ($\sim 30°$) by using a two step etch process or over etch process.[4]

IV. CONCLUSIONS

For unbiased rf magnetron sputtered MoW films the electrical resistivity as a function of tungsten fraction follows a typical Nordheim relationship. The resistivity increases with the addition of solute atoms (tungsten) and it is maximum at ~ 0.5 atomic fraction of solute atoms. Films sputtered at room temperature without substrate bias contained a second metastable phase (β-W) which results in a significantly higher resistivity due to the lattice mismatch between stable α-W and metastable β-W. As sputtering temperature increases, the β-W does not form and the resistivity decreases over the entire composition range relative to the room temperature deposited sample. Thin films deposited with substrate bias had a considerably lower resistivity over the entire composition range and their resistivity as a function of composition obeys a rule of mixture rule. Additionally, in the MoW film deposited with biased sputtering, the β-W phase is not present even at room temperature. From the SEM results, a denser and void-free structure is shown in the microstructure of biased thin films. Additionally, unlike bulk molybdenum and tungsten, biased tungsten films had higher resistivity than biased molybdenum. This phenomenon is consistent with the fact that the dislocation resistivity of tungsten is two orders of magnitude higher than that of molybdenum.

ACKNOWLEDGMENTS

This work was supported in part by the National Institute for Biomedical Imaging and Bioengineering under assignment No. 1-R01EB000433-01, by the Material Sciences and Engineering Division Program of the Department of Energy Office of Science under Contract No. DE-AC05-00OR22725 with UT-Battelle, LLC, and through the Laboratory Directed Research and Development funding program of the Oak Ridge National Laboratory, which is managed for the U.S. Department of Energy by UT-Battelle, LLC.

[1]Y. Kuo, J. Electrochem. Soc. **142**, 2486 (1995).
[2]H. H. Choe and S.-G. Kim, Semicond. Sci. Technol. **19**, 839 (2004).
[3]M. Ikeda *et al.*, SID Int. Symp. Digest Tech. Papers **1995**, 11.
[4]K. Okajima, T. Sato, T. Dohi, and M. Shibata, Vacuum **51**, 765 (1998).
[5]P. Petroff, T. T. Sheng, A. K. Sinha, G. A. Rozgonyi, and F. B. Alexander, J. Appl. Phys. **44**, 2545 (1973).
[6]H. B. Shukovsky, R. M. Rose, and J. Wulff, Acta Metall. **14**, 821 (1966).
[7]L. D. Whitmire and F. B. Brotzen, Trans. Metall. Soc. AIME **239**, 824 (1967).
[8]R. C. Sun, T. C. Tisone, and P. D. Cruzan, J. Appl. Phys. **44**, 1009 (1973).